(4) B. Ekman, C. Lofter, and I. Sjöholm, *Biochemistry*, **15**, 5115 (1976).
(5) I. Ljungstedt, B. Ekman, and I. Sjöholm, *Biochem. J.*, **170**, 161 (1978).
(6) Y. Pocker and J. T. Stone, *Biochemistry*, **6**, 668 (1967).
(7) E. J. Cohn, W. L. Hughes, Jr., and J. H. Weare, *J. Am. Chem. Soc.* **69**, 1753 (1947).
(8) E. W. Davie, C. R. Newman, and P. E. Wilcox, *J. Biol. Chem.*, **234**, 2635 (1959).
(9) G. H. Beaven and F. R. Holiday, *Adv. Protein*, **7**, 319 (1952).
(10) H. Pertoft, L. Philipson, P. Oxelfelt, and S. Höglund, *Virology*, **33**, 185 (1967).
(11) H. Nilsson, R. Mosbach, and K. Mosbach, *Biochim. Biophys. Acta*, **268**, 253 (1972).
(12) R. C. Boguslaski and A. M. Janik, *ibid.*, **250**, 266 (1971).

ACKNOWLEDGMENTS

Supported by the Swedish Board for Technical Development (Project 75-4415), the Swedish Medical Research Council (Project 13X-3126), and the I.F. Foundation for Pharmaceutical Research, Stockholm.

The technical assistance of Mr. Börje Berg is gratefully acknowledged.

Permeability of Interstitial Space of Muscle (Rat Diaphragm) to Solutes of Different Molecular Weights

JEROME S. SCHULTZ ˣ and WILLIAM ARMSTRONG

Received April 7, 1977, from the *Department of Chemical Engineering, University of Michigan, Ann Arbor, MI 48109.* Accepted for publication September 21, 1977.

Abstract □ The transport characteristics of muscle interstitial space were determined using an isolated rat diaphragm preparation. Permeability of the interstitial space for extracellular solutes is one-thirtieth to one-fiftieth that of an equivalent thickness of water. However, most of this low permeability can be accounted for by correcting for the tortuosity and relative volume of interstitial space. The estimated diffusivity of solutes (mol. wt. 100–70,000) in the interstitial space of muscle is only about one-half to one-fifth less than in water alone.

Keyphrases □ Permeability—interstitial space of rat diaphragm muscle to solutes of different molecular weights □ Transport characteristics—interstitial space of rat diaphragm muscle, permeability to solutes of different molecular weights

The prediction of the transport rates at which solutes and drugs cross interstitial space—either from blood to tissue or from tissue to circulation—is dependent on a knowledge of the relative resistances of these regions to transport.

Although several studies focused on the capillary endothelium (1–3), less work has been done on defining the role of the interstitial space and how it affects the net transport rate between blood and tissues. In nonsteady-state experiments using tracers, a temporary interruption in blood flow affected solute transport in a manner attributed to diffusion resistance in the interstitial space (4). By treating muscle with hyaluronidase, the absorption rate of intramuscularly injected dextrans was accelerated (5). Other experiments (6, 7) involved measurement of permeation rates through polyglycon gels prepared to simulate the composition of interstitial polysaccharides; it was suggested that diffusion through muscle tissue might be highly restricted, especially with macromolecules.

The objective of this study was to find the relationship between solute size and solute mobility in the interstitial space of muscle. Tracer solutes were used which, except for tritiated water, are retained in the extracellular space of muscle tissue. And by imposing a dextran gradient across a muscle preparation, the influence of osmotic forces in interstitial transport was evaluated.

Because the diaphragm is constituted of striated muscle and because the flat, sheet-like configuration lends itself to measurements of transient and steady-state transport rates by conventional membrane-testing techniques, the diaphragm of the rat was used in these experiments. This muscle has been used extensively as an experimental preparation in transport studies (8), cellular uptake studies (9), and work on hormonal influences on transport and uptake (10).

EXPERIMENTAL

Rat Diaphragm Preparation—Sprague–Dawley male rats, mostly retired breeders[1], 250–500 g, were injected with 35 mg ip of pentobarbital.

After the abdominal cavity was opened with a midline incision, the vena cava was clamped about 1 cm caudal to the vena caval hiatus. A 1.0-mm longitudinal incision was made in the vessel, and a catheter[2] was introduced and secured with 3-0 silk suture. The thorax was opened just above the sternum, and the thoracic vena cava was tied. The catheter was connected to a syringe pump equipped with a glass 30- or 50-ml syringe, and retrograde perfusion of the diaphragm vascular bed with Krebs–Ringer bicarbonate buffer was begun (11).

The diaphragm was removed by cutting the abdominal wall with scissors just caudal to the costal border, girdling the animal. A similar girdling cut was made just cephalad to the costal rim, and the trunk of the rat was disconnected above and below the diaphragm with bone shears and scissors.

The excised diaphragm, still undergoing retrograde perfusion, was mounted on a rigid, flat, 1.6-mm polycarbonate ring, about 7 cm o.d. and 5 cm i.d., using straight pins at the costal margin which fit into predrilled 1-mm holes in the ring. Once mounted, the diaphragm was either suspended vertically above a specimen dish for the permeability experiments or submersed in a cocktail of buffer, radioactive tracer, and dye for the equilibration experiments.

[1] Spartan Research Animals, Inc., Haslett, Mich.
[2] Intramedic polyethylene tubing PE 160.

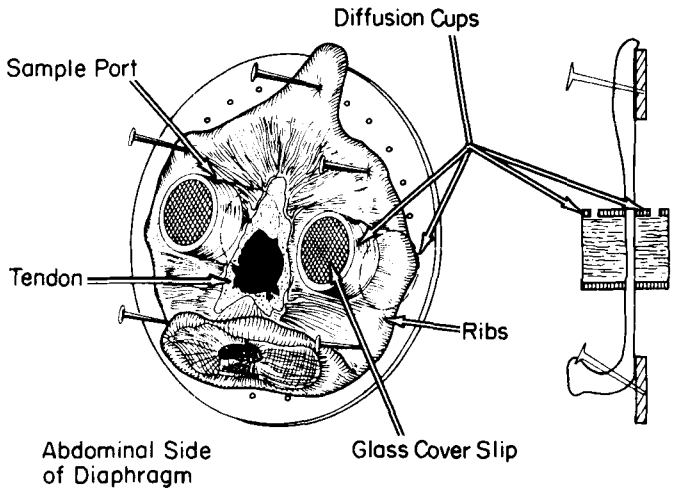

Figure 1—*Schematic diagram of the rat diaphragm preparation for the measurement of solute transport through the interstitial space of muscle. Diffusion cups were affixed to the muscle with a cyanoacrylate adhesive.*

Permeability Measurements—In the permeability experiments, two sets of matched cups were juxtaposed and secured on the diaphragm walls with adhesive (Fig. 1). The cups were fabricated from carefully sliced segments of polyvinyl chloride tubing[3] (12.7 mm i.d., 2.4 mm wall thickness); to one end of the sliced tube, a microscope slide coverglass was attached with a cyanoacrylate[4] adhesive. The open, cut surface of the cup was mounted directly on the diaphragm muscle with another cyanoacrylate[5] adhesive so that each pair of cups was in alignment, with the diaphragm constituting the partition between the chambers.

This method of attachment of the diffusion chambers precludes damage to muscle or vasculature due to clamping or other pressure-dependent attachments. The seal between the end of the plastic tubing and the tissue surface is remarkably strong and leakproof. When carefully applied, the adhesive does not invade onto the diaphragm surface within the chamber. The area of diaphragm available for diffusion may be confidently measured. In other published studies (8) where clamping arrangements were used, damage to tissue on the periphery of the chamber may have extended 1 mm beyond the cage; if so, and if the chamber was 1 cm in diameter, the damaged area may have included 20% of the experimental area.

Through 0.5-cm portals in the tops of the diffusion chambers, test solutions were introduced and monitored.

With the two sets of chambers, *i.e.*, one on the hepatic side and one on the splenic side, it was possible to run experiments either in duplicate or with a control and a variation on the same preparation.

Before test solutes were added to the chambers, the diaphragm preparation was allowed to come to equilibrium at room temperature (about 22°) with buffer solution in all cups for about 10 min. Tracer solutes were then added to the abdominal chambers, and the chambers on the pleural surface were monitored periodically for diffused materials.

Measurement of Interstitial Space—After the diaphragm was excised from the anesthetized rat and perfused 10 min with Krebs–Ringer bicarbonate buffer, it was ring mounted with pins and submersed in a solution containing the radioactive tracer of the solutes to be tested, 0.03% patent blue, and 1.5% bovine serum albumin in Krebs–Ringer bicarbonate buffer.

At intervals from 5 to 60 min, the mounted diaphragm was removed from the bath and placed on a rubber platform; a disk of muscle tissue, 0.95 cm in diameter, was excised with a tubular knife. Immediately after cutting out the tissue sample, the diaphragm was returned to the bath.

The tissue disk was rinsed 2 sec in 10 ml of 0.9% NaCl, blotted quickly on filter paper, and placed on a square of aluminum foil (1.5 × 1.5 cm) for weighing. It was then transferred to a screw-capped test tube (13 × 100 mm) containing 1.0 ml of 1.5% bovine serum albumin in Krebs–Ringer bicarbonate buffer and stored at 5° overnight to extract the patent blue.

[3] Tygon.
[4] Eastman 910.
[5] Formula 9, Johnson & Johnson.

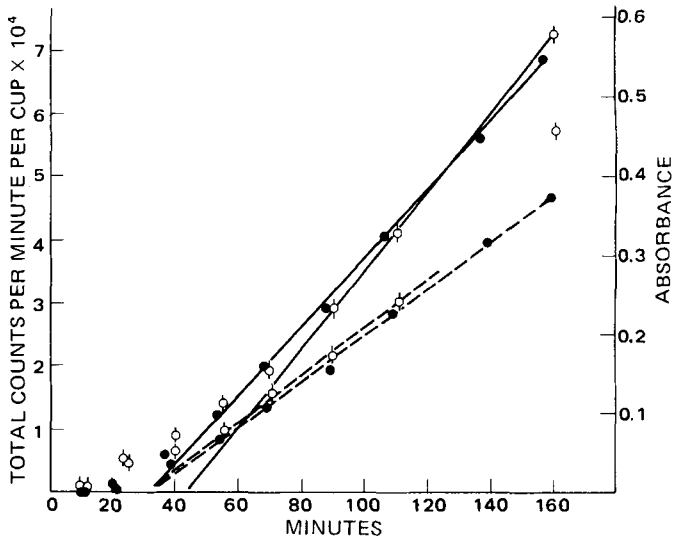

Figure 2—*Appearance of inulin and patent blue in the downstream chamber after the addition of tracers to the upstream chamber. Diffusion rates for two sections of the same diaphragm were slightly different, but relative transport rates for different solutes were about the same. Key: ○, ^3H-inulin; and ●, patent blue. Solid and dashed lines are for the individual sections of the diaphragm.*

On the following day, the tissue disk was transferred to a scintillation vial containing 1.0 ml of tissue solubilizer[6]. After digestion, 10 ml of toluene scintillant was added; the radioactive component in the tissue was measured by a scintillation counter.

The solution in which the disk had soaked was transferred to a spectrophotometric cell, and the absorbance of patent blue at 640 nm was recorded. An aliquot of this liquid component was removed and counted in the scintillant.

Internal standards were added when appropriate to compensate for the quenching effects of patent blue and solubilizer.

Analytical Methods—Absorbance measurements were obtained by transferring the contents of the diffusion chamber with a Pasteur pipet into a 1.0-ml spectrophotometer cell and reading the absorbance at 640 nm with a spectrophotometer. Radioactivities were measured by removal of aliquots, usually 10 μl, with disposable micropipets and counted in a liquid scintillation system.

Solutions and Materials—The Krebs–Ringer bicarbonate buffer had

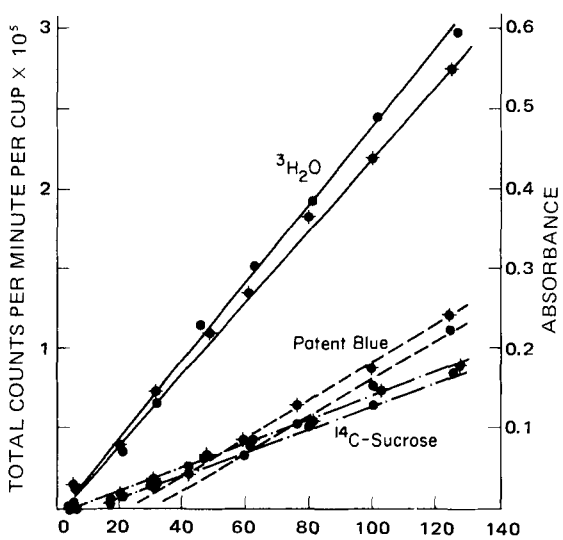

Figure 3—*Diffusion of ^3H-water, ^{14}C-sucrose, and patent blue across the rat diaphragm. One downstream chamber contained dextran T70 (●), and the other did not (-●-). The dextran osmotic pressure gradient does not augment transport rates.*

[6] Soluene 100, Packard.

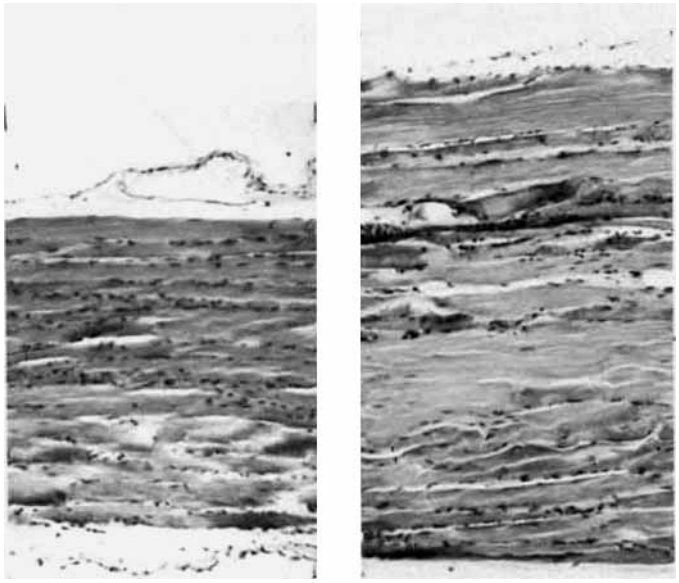

Figure 4—*Histological sections of rat diaphragm before (left) and after (right) a 3-hr diffusion experiment. Sections were made parallel to fiber length. Spacing between fibers was virtually unchanged by experimental procedure. (These sections were from two different animals.)*

the following composition: 0.7% NaCl, 0.035% KCl, 0.028% $CaCl_2$, 0.016% KH_2PO_4, 0.029% $MgSO_4 \cdot 7H_2O$, and 0.21% $NaHCO_3$.

^{131}I-Serum albumin[7] was dialyzed extensively to remove any free iodide. Patent blue violet[8], bovine serum albumin[9] (fraction V), ^{35}S-sodium sulfate[10], ^{14}C-D-sucrose[10], ^{3}H-methoxyinulin[10], ^{3}H-water[10], and dextrans[11] were used as received.

RESULTS

In Figs. 2 and 3, which show typical diffusion patterns, it is evident that before a steady-state gradient is established through the tissue, there is a lag period during which binding sites and dead-ended volumes are saturated. After this lag time, the flux through the tissue is essentially constant, indicating that the system has achieved a pseudosteady state under these experimental conditions. For slowly diffusing molecules such as albumin, the curve remains straight for several hours. For rapidly diffusing substances such as water, the permeation curve soon plateaus since both chambers equilibrate with tracer.

Generally, the lag time increases with the size of the solute species. This information can be used to estimate tortuosity and dead-end porosity (8, 12), but such calculations are thought to be very model dependent (13). For the analysis of the data presented here, only the constant slope portion of the permeation curve, or the pseudosteady-state portion, was used.

In all permeation experiments, patent blue was used as an extracellular reference marker. This dye does not bind to plasma proteins or tissue membranes (14). Besides providing an immediate indication of leaks within the diaphragm–chamber preparation, the dye also provided a convenient colorimetric control while other test solutes were measured by radiotracer techniques. In some experiments, two different isotopic tracers along with patent blue were used to obtain three relative diffusion rates from a single muscle preparation.

Figure 2 shows the diffusion results of duplicate experiments on the same diaphragm with patent blue and inulin as the tracer solutes. Whereas the average diffusion rates for the two chambers were slightly different, the inulin transport rate relative to patent blue transport was the same. Thus, by normalizing diffusion rates in relation to a reference molecule, the minor variations in tissue properties that may occur from one area of a tissue preparation to another or from animal to animal are effectively eliminated.

Diaphragm thickness measurements were made with an electronic contact micrometer before and after each experiment. The diffusion chambers were emptied and gently removed without damage to the diffusion surface area. The thickness of the diaphragm in this region increased by about 20% over 3 hr.

[7] Prepared by the Nuclear Pharmacy Department, University of Michigan.
[8] Color index 42045, Sigma Chemical Co.
[9] Sigma Chemical Co.
[10] New England Nuclear Corp.
[11] Pharmacia Fine Chemicals.

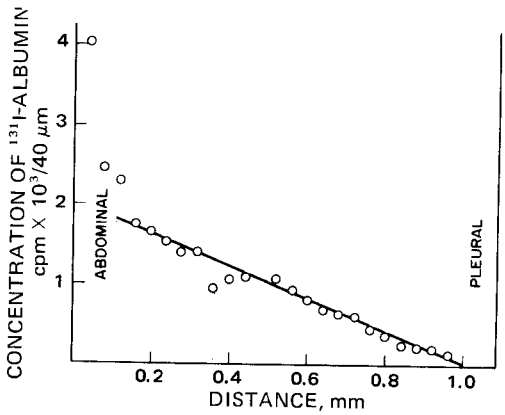

Figure 5—*Concentration profile of ^{131}I-albumin across a rat diaphragm after a steady-state permeation rate was attained. The tissue was quickly frozen and then sectioned parallel to the surface of the diaphragm.*

To determine whether the interstitial space underwent significant expansion during the experiments, tissue samples from control and experimental diaphragms were processed for histological comparison. The increase in tissue thickness during the experiment was caused by an apparent swelling of the muscle fibers rather than by the accumulation of liquid in the interstitial space. Photographs of histological samples are shown in Fig. 4.

The fact that the transmuscle flux remained constant for several hours suggests that the extracellular structure of the diaphragm remains stable at least during the experiment. If the interstitial space were to become edematous, solute mobility would increase, as reflected by an increase in the upward curvature of the lines in Figs. 2 and 3.

Portions of diaphragms used for the diffusion experiments were excised and analyzed for the distribution of tracer across the sheet of muscle. These sections were quickly frozen on a precooled slab and were sectioned longitudinally (parallel to the surface of the diaphragm) with a cryostatic microtome. Series of these sections were pooled in counting vials so that the profile of radioactivity across the thickness of the diaphragm was obtained.

A typical distribution is shown in Fig. 5. In this experiment, after achieving a steady-state flux, the distribution of ^{131}I-albumin was measured. The concentration of labeled albumin was generally linear from the abdominal to the plural surface; the amount of scatter found on the abdominal surface was attributed to technical problems in alignment of the microtome blade exactly with the diaphragm surface.

Linear concentration profiles are consistent with simple passive diffusion; other transport processes, such as bulk flow or carrier-mediated flow, are usually nonlinear. If the mesothelium that lines the pleural and abdominal surfaces of the diaphragm constituted a significant permeability barrier, discontinuities in the concentrations of radioactivity would have been found at both surfaces. But the tracer concentration at the pleural surface was essentially the same as in the downstream diffusion chamber, a value close to zero. At the abdominal surface, the radioactivity per unit volume of muscle was about 5% of the concentration in the upstream diffusion chamber. This finding is consistent with independent equilibrium measurements of albumin space in the diaphragm, which showed that about 8% of the muscle is available to albumin (Table I).

Boundary Layer Resistance—The fluid in the chambers affixed to the diaphragm in these experiments was not subjected to any mixing beyond that caused by density gradients. Therefore, the resistances at the tissue–fluid interface, *i.e.*, the unstirred boundary layer, would be expected to be large.

These diffusion resistances were measured by substituting a microporous filter for the diaphragm; this membrane was previously dipped in dilute agar, and then the diffusion cups were affixed by clamps. Agar coating was done to prevent bulk flow through the filter due to slight differences in liquid level. Transport rates of various solutes across the agar membrane were measured.

The fluxes of ^{3}H-water, ^{14}C-sucrose, and patent blue through the membrane were measured using the same procedures as in the diaphragm experiments. The permeability of the boundary layers, P_{layers} (one on each side of the membrane), for each solute was calculated from the series

Table I—Estimate of Solute Diffusivities in Rat Diaphragm

Solute	Permeability Rat Diaphragm, cm/sec × 10^6	Void Space, ψ	Estimated Tortuosity, τ	Diffusivity: Calculated in Diaphragm, cm^2/sec	Diffusivity: in Water, cm^2/sec	Ratio
Water	55.6	0.79 ± (3)[a]	1.5	6.8×10^{-6}	23.0×10^{-6}	0.30
Sodium sulfate	4.72	0.20 ± 0.008 (3)	2.5	3.6×10^{-6}	11.0×10^{-6}	0.33
Sucrose	2.79	0.31 ± 0.08 (4)	2.5	1.4×10^{-6}	5.1×10^{-6}	0.28
Patent blue violet	1.55	0.30 ± 0.08 (13)	2.5	0.82×10^{-6}	3.1×10^{-6}	0.27
Inulin	0.996	0.31 ± 0.09 (3)	2.5	0.51×10^{-6}	2.4×10^{-6}	0.21
Albumin	0.178	0.08 ± 0.04 (10)	2.5	0.36×10^{-6}	0.7×10^{-6}	0.52

[a] Numbers in parentheses indicate the number of observations.

resistant equation:

$$\frac{1}{P_{obs}} = \frac{1}{P_{layers}} + \frac{1}{P_{membrane}} \quad \text{(Eq. 1)}$$

where the individual permeability values were obtained from the experimental observations:

$$P_{obs} = \frac{(\Delta C/\Delta t)V_d}{A(C_u - C_d)} \quad \text{(Eq. 2)}$$

where $(\Delta C/\Delta t)$ is the slope of the lines shown in Figs. 2 and 3, V_d is the volume of the downstream chamber, A is the area available for diffusion, and $(C_u - C_d)$ is the concentration difference of solute between the upstream and downstream compartments.

The permeability of the microporous filter for each solute was estimated from the known properties of the filter (15): thickness = 0.0160, porosity = 0.8, tortuosity = 1.2, and $P_{membrane} = (D \times 0.8)/(0.016 \times 1.2)$, where D is the diffusion coefficient of the solute in water.

As shown in Fig. 6, the boundary layer permeability increases with solute diffusivity, as expected. The slope of the line is about 0.33, so $P_{layers} = \alpha D^{1/3}$ for this experimental apparatus. This 0.33-power dependency of boundary layer permeability differs from the value of 0.6 obtained in experiments where the solutions were mechanically stirred (16). Values of boundary layer permeability for each solute tested can be obtained by extrapolation (Fig. 6). For each solute except ^{3}H-water, the boundary layer permeability was considerably greater than the permeability of the diaphragm, so only very small corrections were necessary to make the permeability estimates for muscle.

Effect of Osmotic Gradient on Transport—A series of experiments was conducted to determine whether solute transport through muscle tissue was augmented by an osmotic gradient. An osmotic differential was achieved by preparing the downstream buffer to contain 4.5% dextran T70, a concentration that has an effective osmotic pressure of 52 cm H_2O. If the interstitial space of muscle consists of a very dense meshwork of carbohydrate polymers relatively impermeable to large molecules (6), one would expect the dextran to cause an osmotic water flow from upstream to downstream chambers. The apparent permeation rate would be higher because of the drag effect of the water flow on solute molecules.

Experiments did not support this expectation. Most of the comparative data on this point, about 35 experiments, were obtained with patent blue as the tracer substance. The mean permeability of patent blue across the diaphragm with a dextran gradient was $1.4 \pm 0.7 \times 10^{-6}$ cm/sec, which is not significantly different than the mean value of $1.3 \pm 0.4 \times 10^{-6}$ cm/sec obtained when no dextran was added to the downstream chamber. Similar results were obtained with the other solutes (Table II). For osmotic substances of the size of dextran T70, the matrix of polymers within the interstitial spece apparently is not tight enough to induce osmotic flow or, in other words, dextran T70 is not an oncotic agent for the rat diaphragm.

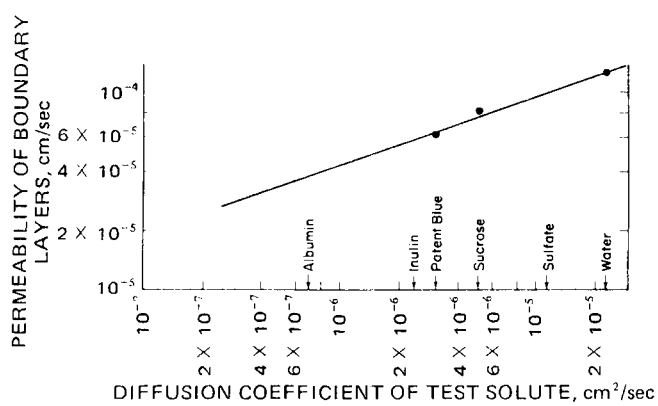

Figure 6—*Boundary layer resistances for various solutes. Measurements were made using ^{3}H-water, ^{14}C-sucrose, and patent blue. Other values were determined by interpolation.*

Permeability of Rat Diaphragm to Solutes—Since there was no statistical difference between permeation rates across the diaphragm with and without a dextran gradient, all data were pooled and used to obtain mean estimates of the permeability rates for each solute.

As mentioned, patent blue was a control solute in each experiment. Mean values for permeabilities were estimated by first relating the test solute permeability to its patent blue control and then averaging the data.

Based on the steady portion of the diffusion curves (Figs. 2 and 3), P_{obs} for each solute was calculated according to Eq. 2. For each solute, the $P_{solute}/P_{patent\ blue}$ ratio was calculated and averaged over all experiments for that solute; these mean values are given in the second column of Table III. The mean $P_{solute}/P_{patent\ blue}$ ratio was multiplied by the grand mean permeability for patent blue, 1.51×10^{-6} cm/sec, to obtain the estimate for the mean permeability of diaphragm muscle to each solute, $\overline{P}_s$. Mathematically:

$$\overline{P}_s = \left[\frac{\sum_1^i P_{si}/P_{PBi}}{i}\right]\left[\frac{\sum_1^n P_{PBn}}{n}\right] \quad \text{(Eq. 3)}$$

where i is the number of experiments with an individual solute (s), and n is the total number of observations of patent blue (PB) permeability. Each mean value for observed solute permeabilities was then corrected for the boundary layer permeability of each solute by Eq. 1 to obtain the permeability of the diaphragm for each solute given in the fourth column of Table III. The correction for boundary layer effects was less than 5% for all solutes except ^{3}H-water; therefore, the accuracy of the correction factors obtained from Fig. 6 is not critical to the results.

DISCUSSION

Of the solutes used, all except ^{3}H-water are confined to the extracellular space. Because of its facile transport across cell membranes, water penetrates muscle through both extracellular and intracellular paths. Therefore, the measured permeability of ^{3}H-water reflects some average resistance of the interstitial space and intracellular space.

The other five solutes are presumed to diffuse through the interstitial space alone, so their permeation rates can be compared meaningfully. In these experiments, the permeability of the interstitial space decreased with the increasing size of the probe solute by a factor of 26 (4.7/0.18),

Table II—Effect of Dextran T70 Gradient on the Permeability of Rat Diaphragm for Various Solutes (Paired Observations)

Solute	Permeability Control / Permeability with Dextran Gradient
^{3}H-Water	0.9 ± 0.4 (4)[a]
^{35}S-Sodium sulfate	1.0 ± 0.2 (4)
Patent blue violet	1.0 ± 0.3 (8)
^{131}I-Albumin	1.5 ± 0.4 (4)

[a] Numbers in parentheses indicate the number of observations.

Table III—Average Permeabilities of Diaphragm to Solutes

Solute	Permeability Relative to Patent Blue, P_s/P_{PB}	Mean Permeability, cm/sec × 10^6	Permeability (Corrected for Boundary Layers), cm/sec × 10^6	Permeability of Diaphragm Relative to Water Layer, $P_{diaphragm}/P_{water\ layer}$
Water	25.5 ± 9.7 (10)[a]	38.5	55.6	0.16
Sodium sulfate	2.99 ± 1.7 (5)	4.51	4.72	0.028
Sucrose	1.79 ± 0.55 (16)	2.70	2.79	0.036
Patent blue violet	(1.00)	1.51 ± 0.71 (56)	1.55	0.033
Inulin	0.65 ± 0.23 (13)	0.98	0.996	0.027
Albumin	0.117 ± 0.042 (17)	0.176	0.178	0.017

[a] Numbers in parentheses indicate the number of observations.

as expected, based on decreasing diffusion coefficients with increasing molecular diameter. The inherent effect of molecular mobility can be compensated for by comparing the measured muscle permeabilities to the permeability of a water layer of the same thickness as the rat diaphragm.

By using the equation $P_{water} = D_s/\delta$, where D_s is the diffusivity of the solute in water (Fig. 6) and δ is the equivalent water layer thickness, 0.065 cm, the $P_{diaphragm}/P_{water}$ ratio was calculated for each solute. The results are shown in the last column of Table III. The range of this ratio for the extracellular solutes is reduced to a factor of about 2, indicating that molecular mobility, *i.e.*, diffusivity, is one main parameter controlling transport in the interstitial space.

These data also show that, in the molecular weight range of 100–70,000, there is no major sieving effect with increases in molecular size within the interstitial space. This result is in contrast to the marked sieving effects attributed to the endothelial lining of capillaries (1).

However, the absolute values of the permeability ratios show that transport through the diaphragm is 30–50 times slower than an equivalent layer of water. As discussed below, the relatively slow transport through muscle may, to some extent, be imputed to the heterogeneous structure of muscle. Whatever the cause, the mean measured permeabilities should provide a sound basis for the estimation of steady-state rates at which extracellular solutes, drugs, hormones, and proteins transport across muscle tissue.

Muscle microanatomy has been studied in great detail. It is convenient to visualize a model of interstitial space as a complex network of voids intermingled with closely packed cylinders of muscle. The diffusional tortuosity of this space has not been determined accurately. Neither have accurate measurements been made of that fraction of the interstitial space which is dead ended, areas that, from the point of view of permeability, are cul-de-sacs. So, admittedly, to estimate diffusion coefficients of solutes in the interstitial space based only on flux measurements is hazardous. However, such estimates may be of value in revealing the relative influences on transport of tortuosity and void space.

The following model was assumed for permeability through a porous material:

$$P = \frac{D\psi}{L\tau} \qquad \text{(Eq. 4a)}$$

or:

$$D = \frac{PL\tau}{\psi} \qquad \text{(Eq. 4b)}$$

where D is the diffusion coefficient in the interstitial space, ψ is the void fraction, L is the geometric thickness of the tissue, and τ is the tortuosity of the extracellular path.

The calculations for the diffusion coefficient of each solute in muscle are summarized in Table I, with the fraction of total muscle volume accessible to each solute given in the third column. For water, the void volume was determined by drying; all other values were determined by equilibrium uptake experiments. The void volume for water is much higher than the others because it penetrates muscle cells as well as the extracellular fluid. Albumin, probably because of steric hindrance, appears to have a significantly smaller distribution space than the other extracellular solutes. Tortuosity estimates for muscle tissue ranging from 1.5 to 5.0 have been made based on the lag time to achieve pseudo-steady-state diffusion rates (8, 12, 13). Larger tortuosities are expressed for larger molecules because of steric interference in the transport of large particles (17).

Because it moves through parallel pathways, a low value of tortuosity was assigned to water; a moderate value of 2.5 was assigned to all other solutes. Estimates for the diffusion coefficients of the various probe solutes within interstitial space were calculated using Eq. 4*b* with a mean value of 0.065 cm for L. These values are listed in Table I, and the calculated diffusivities are compared to the diffusivities of these solutes in water. Overall, it appears that the mobility of solutes in interstitium is 0.2–0.5 of that in water and that the reduced mobility is not strongly correlated with molecular size.

If the use of Eq. 4*b* with the estimates of tortuosity and void fraction is appropriate, a major part of the low permeability values for whole muscle can be explained by these geometric factors. The remaining one-half to one-fifth reduction in mobility as compared to water may be due to a higher viscosity of the interstitial fluid and/or some diffusion hindrance due to the porous nature of the tissue (16).

Using fluorescence microscopy, Nakamura and Wayland (18) estimated the diffusion coefficient for albumin in rat mesentery and found it to be fairly close to its value in water. Their conclusion that substances move fairly freely within the interstitial space of tissues is corroborated by the present findings.

REFERENCES

(1) J. R., Pappenheimer, E. M. Renkin, and L. M. Borrero, *Am. J. Physiol.*, **167**, 13 (1951).

(2) D. Garlick and E. Renkin, *ibid.*, **219**, 1595 (1970).

(3) N. Simionescu, M. Simionescu, and G. Palade, *Thromb. Res. Suppl. 2*, **8**, 257 (1976).

(4) C. Crone and D. Garlick, *J. Physiol. (London)*, **210**, 387 (1970).

(5) R. Sund and J. Schou, *Acta Pharmacol. Toxicol.*, **23**, 194 (1965).

(6) T. C. Laurent, *Pfluegers Arch., Suppl.*, **336**, S21 (1972).

(7) B. N. Preston and J. M. Snowden, *Biopolymers*, **11**, 1627 (1972).

(8) N. Brookes and D. Mackay, *Br. J. Pharmacol.*, **41**, 367 (1971).

(9) D. M. Kipnis and C. F. Cori, *J. Biol. Chem.*, **224**, 681 (1957).

(10) T. Clausen, in "Current Topics in Membranes and Transport," vol. 6, F. Bronner and A. Kleinzeller, Eds., Academic, New York, N.Y., 1974, pp. 189–225.

(11) F. D. Hollanders, *Comp. Biochem. Physiol.*, **26**, 907 (1968).

(12) E. Page and R. S. Bernstein, *J. Gen. Phys.*, **47**, 1129 (1964).

(13) M. Suenson, D. R. Richmond, and J. B. Bassingthwaighte, *Am. J. Physiol.*, **227**, 1116 (1974).

(14) C. A. Wiederhelm, M. Show, T. Kehl, and J. Fox, *Microvasc. Res.*, **5**, 243 (1973).

(15) S. Suchdeo and J. S. Schultz, *Biochim. Biophys. Acta*, **352**, 412 (1974).

(16) R. E. Beck and J. S. Schultz, *ibid.*, **255**, 273 (1972).

(17) H. E. Schultze and J. Heremans, "Molecular Biology of Human Proteins," vol. 1, Elsevier, Amsterdam, The Netherlands, 1966.

(18) Y. Nakamura and H. Wayland, *Microvasc. Res.*, **9**, 1 (1975).

ACKNOWLEDGMENTS

Supported in part by National Institutes of Health Grant GM15152 and Research Career Development Award 1-K4-GM-8271 to J. S. Schultz.